Journal of Polymers and the Environment
https://doi.org/10.1007/s10924-023-03043-1

ORIGINAL PAPER

Soft Robotic Actuation Facilitated by Polypyrrole Coated-Sulfonated Polyvinyl Alcohol-Graphene Oxide-ZnO Network-Based Nanocomposite Membranes

Syed Khalid Mustafa[1] · Meshari M. H. Aljohani[1] · Ali Hamzah Alessa[1] · Hatem A. Al-Aoh[1] · Mahmoud A. Abdelaziz[1] · Noha Omer[1] · Asma Obaidallah Alatawi[1] · Faheem Ahmad[2]

Accepted: 24 August 2023

Abstract

This study presents the synthesis of polypyrrole coated over sulfonated polyvinyl alcohol and graphene oxide-nanosized ZnO network-based nanocomposite actuators (*SPVA/GO/ZnO-Nps/PPy*). The solution casting approach was used to create the membrane. $HO_3SC_6H_3$-1,2-$(CO_2H)_2$ was used as a sulfonating agent during the sulfonation process of polyvinyl alcohol. A polypyrrole coating is done on a sulfonated polyvinyl alcohol and graphene oxide-nanosized ZnO network substrate using an aqueous chemico-oxidation polymerization process with in-situ polypyrrole synthesis. The consistent network that can block water loss was also revealed using scanning electron microscopy. An adequate ion-exchange potential of 1.79 meq g^{-1} was demonstrated by the dry membrane sulfonated polyvinyl alcohol graphene oxide-nanosized ZnO networks with polypyrrole coatings. It was observed that the membrane's absorption capacity at 45 °C was around 80.45% after roughly 24 h of dousing. Excellent proton conductivity of 1.69×10^{-3} Scm^{-1} was observed by the polypyrrole coating of the nanocomposite membrane. The membrane's capacity to lose water was estimated to be around 37.8% for 10 min, at 6 V. In addition, at 4 V, the electro-mechanical characterization revealed a maximum tip displacement of 15.5 mm. In comparison to earlier published expensive polymer-based membranes, the claimed nanocomposite membrane improved water-absorption, ion-exchange capacity, and ionic-conductivity enhanced the electrical characteristics with good performance of tip deflection. The development of a microgripper based on a polypyrrole coated over sulfonated polyvinyl alcohol and graphene oxide-nanosized ZnO network-based nanocomposites membrane (*SPVA/GO/ZnO-Nps/PPy*) has a lot of potential for use as soft robotic actuators.

Keywords Sulfonated polyvinyl alcohol · Polypyrrole · ZnO Networks · Soft actuators · Microgrippers

Introduction

In recent years, ionic polymer-metal composites (IPMCs) have attracted a lot of attention as one of the best platforms for electroactive active polymers, especially in the fields of soft robotics, IPMC sensors, and IPMC artificial muscles, among others [1–7]. Due to their notable attributes, including ease of preparation, light in weight, flexibility, high sense, and durability, these are servicing impulsive exploitations [8]. It is indeed intriguing to note how IPMC-based actuators only need a relatively small level of external electrical activity, ranging to ≥ 6 V, to function in both in air and water environments [9]. In a physiologically regulated environment, IPMCs have been found to bend more significantly than usual robotic actuation materials [10]. In light of this, IPMCs are used in a broad variety of applications, such as actuators with tactile virtual reality (VR), bio-inspired robot launching systems, and cardiac (implantable) compression and assist devices through IPM composites (IPMC) [11–14].

IPMCs are typically comprised of a newly produced membrane of permeable polymers with ionic-exchange properties that is bonded on both sides with a metal electrode made of Pt/Au, with water serving as the inner phase

✉ Faheem Ahmad
faheem.bt@amu.ac.in

Asma Obaidallah Alatawi
a.oalatawi@ut.edu.sa

[1] Department of Chemistry, Faculty of Science, University of Tabuk, 71491 Tabuk, Saudi Arabia

[2] Department of Botany, Aligarh Muslim University, Aligarh 202002, India

Published online: 23 September 2023

for cationic dissociation/transport of metals [15–17]. This causes the cathodic portion of the polymer membrane to lengthen when an electric voltage is applied, which stresses the IPMC membrane's cation-rich region and causes it to bend in the anodic direction. But in dry settings, cross-linked-cations are static. However, in moist environments, cations are surrounded by water molecules, which make the entire membrane film movable due to hydration. As an outcome, the cations' mobility inside the IPMC layer is caused by their encapsulation in water molecules. A number of perfluorinated sulfonic acid (PFSA) ionomers are part of a class of ion-conductive polymers known for their exceptional ion conductivity and chemical-mechanical stability, are commercially available, and are used in IPMCs actuator applications due to their potent physico-chemical properties [5, 18–26]. Owing to its inherent advantages, including their rapid proton conducting capability and thermo-chemo-mechanical stabilities, perfluorinated IPMC membranes sold under the trade name Nafion are commonly utilised as actuators and dynamic sensors. Due to high water evaporation and the pricey manufacturing of Nafion membrane, researchers around the world are currently seeking for alternatives to these traditional membranes [27–30].

The aforementioned problems might be addressed by switching to non-perfluorinated films from typical Nafion substrates [23, 31–38]. Researchers are putting a lot of effort into creating non-perfluorinated membranes that are economical, have improved water holding even at elevated temperatures, and are simple to produce. In order to substitute perfluorinated ionic polymers as bending actuators, standard ionic polymeric materials, such as styrene and vinyl alcohol, etc., that may incorporate sulfonation/carboxylation, have been used in the past [35, 39–46].

The biggest drawback of IPMC actuators, on the other hand, is their back-drivable characteristics, which restrict bending movement and resonance frequency/amplitude parameters. In addition, rapid performance deterioration, back relaxation behaviour, and prolonged processing time are produced by excessive water loss from IPMC membranes in response to an electric field that is applied throughout the membrane. These factors are crucial to IPMC actuator problems [47, 48].

The incorporation of nanoscale metals or metal oxides may improve the desired features of IPMC, according to several studies being conducted in the emerging field of nanomaterials. So, in order to modify the essential properties of the base polymeric materials using only a minuscule proportion of multi-walled carbon nano-tube (MWNT), Heo et al. produced a MWNT/ionomeric electroactive active polymer (EAP) nanocomposite that could demonstrate capabilities notably different from their bulk scale equivalents. Similar to this, other studies were presented to develop IPMC blended with nanomaterials with desirable properties [49–54].

With the foregoing discussion in mind, this study involved the development of an IPMC nano-membrane composed of non-perfluorinated sulfonated polyvinyl alcohol (SPVA), graphene oxide (GO), nanosized ZnO network (ZnO-Nps), and polypyrrole (PPy) nanocomposites, resulting into a nano-composite known as (*SPVA/GO/ZnO-Nps/PPy*).

The purpose of conducting polymer coating over a traditional IPMC actuator is to enhance the actuator's performance by reducing the creation of membrane surface fissures. Henceforth, the development of IPMC nano-membranes was primarily focused on enhancing the desired actuator performance characteristics compared to IPMC actuators that are currently available. Using the sulfonated non-perfluorinated ionic polymers, IPMC actuators with extended response times and back relaxation have been created. Additionally, it was believed beneficial to develop an IPMC based on a nano-membrane called (*SPVA/GO/ZnO-Nps/PPy*) to enhance the properties of the actuators. As a result, the manufactured nano-composite membrane (*SPVA/GO/ZnO-Nps/PPy*) can be a practical and trusted choice for the creation of novel actuators as well as for prospective industrial utilizations.

Experimental

Materials

Merck KGaA (Darmstadt, Germany) provided the chemicals ($Zn[Ac]_2{\cdot}2H_2O$ and NaOH) for the synthesis process of nanosized ZnO network (*ZnO-Nps*). The capping agent, cetyl trimethyl ammonium bromide, CTAB, was obtained from LobaChemie Pvt Ltd (Mumbai, India). Borosil Glass Works Limited (Mumbai, India) provided the glassware used during the process, and de-mineralized water was used throughout the synthesis. Polyvinyl alcohol from CDH from India, 4-sulfophthalic acid (a 50% solution in water) and graphene oxide, were sourced from Sigma–Aldrich Chemie Pvt. Ltd. from USA. Aniline monomer ($C_6H_5NH_2$) was procured from Thermo Fisher Scientific Pvt. Ltd. in India, while Merck Specialties Pvt. Ltd., Germany provided potassium peroxydisulfate ($K_2S_2O_8$). All reagents were used as received without any additional purification.

Methodology

Instrumentation

A Nicolet iS50 FT-IR instrument was used to conduct Fourier transform infrared spectroscopy (FTIR) over the wavelength range of $4000-400\ cm^{-1}$, in order to identify the material's functional group. To ascertain the crystallinity of the membrane, X-ray diffraction analysis (XRD) was

carried out using the Rigaku Smart Lab X-ray diffractometer. SEM was used on a copper grid coated with carbon paper with an operating voltage of 200 kV using a JSM 6510 LV equipment made by JEOL in Japan to examine the surface morphology of the produced membrane. The elemental analysis was carried out using energy dispersive X-ray (EDX) spectroscopy. Furthermore, the potentiostat/galvanostat device (PGSTAT 302 N) from Autolab, Luzern, Switzerland, has the ability to manage high levels of electrical current and can operate up to a maximum compliance voltage of 30 volts, with a bandwidth of 1MHz. Its design is specifically optimized for the application of electrochemical impedance spectroscopy. Additionally, a magnetic stirrer, electronic digital balance, pH meter and electric oven were employed in the process of drying, measuring, and analyzing the fabricated composite membranes.

Fabrication of Nanosized ZnO Network (ZnO-Nps)

As per *Khan et al.*, to prepare the nanosized ZnO network (ZnO-Nps), a flat-bottomed flask containing de-mineralized water was placed on a magnetic stirrer and heated. Then, 0.2 g of CTAB was added to the water, followed by the addition of 21.94 g (5%) of $Zn[Ac]_2{\cdot}2H_2O$ from a 100 mL solution. While stirring, NaOH solution was slowly added drop-wise to the mixture until the colloidal solution became milky in appearance. The mixture was then cooled, centrifuged, and dried at room temperature. De-mineralized water and methanol were used to wash the fabricated nanosized ZnO network (ZnO-Nps) sample. No special treatment was required during the synthesis process, and the resulting nanosizes were stored for further analysis [55].

Characterization of Nanosized ZnO Network (ZnO-Nps)

The X-ray diffractometer was used to examine the crystal structure and phases of the nanosized ZnO network (referred to as "ZnO-Nps"). The instrument used a monochromatic X-ray beam filtered with nickel to produce Cu-Kα radiation, which was scanned in the 2θ range of 10°–80° with a step size of 0.01° and a scanning rate of 0.02 steps/second. The X-rays were generated with a voltage of 40 kV and current of 40 kA. The size of the *ZnO-Nps* crystallites (referred to as "D") was determined using the Debye–Scherrer equation, which was applied to the most intense peak (101) observed in the X-ray diffraction pattern as:

$$D = \frac{k\lambda}{\beta cos\theta} \tag{1}$$

In this context, the symbol "k" represents the shape factor or proportionality constant, which has a numerical value of 0.9. The symbol "λ" represents the X-ray wavelength emitted by Cu-Kα, which has a specific value of 1.54178 Å. The symbol "β" refers to the diffraction peak's full width at half maximum, measured in radians. Finally, the symbol "θ" refers to Bragg's angle, which is measured in degrees [56].

Fabrication of SPVA/GO/ZnO-Nps Nano-Composite Membrane

To make the ionomer, 4 gm of polyvinyl alcohol were completely dissolved after being agitated for 6 h at 60 °C in 100 ml of de-mineralized water. In order to sulfonate the solution, 4 ml of 4-sulfophthalic acid were added to the clear solution after it had been stirred continuously for 2 h at 60 °C. The sulfonated polyvinyl alcohol solution was agitated further for 10 h at 50 °C. Next, in the prepared solution, 2 ml of GO (graphene oxide) suspension were introduced while being continuously stirred for a duration of 1 h at a temperature of 60 °C. This was followed by ultrasonic treatment, which was carried out for up to 1 h. Afterward, 0.02 g of the previously prepared *ZnO-Nps* were added to the final solution and subjected to ultrasonic treatment for up to 1 h.

Preparation of the Reagent Solutions

An aqueous solution of ferric chloride at a concentration of 0.1 M and a pyrrole solution at a concentration of 33.33% (v/v) are both prepared using de-mineralized water. The $FeCl_3$ solution is then slowly added, drop by drop, to the pyrrole solution with continuous stirring in a ratio of 1:1. As a result of this, the $FeCl_3$ oxidizes the pyrrole, leading to the formation of polypyrrole and giving rise to a greenish–black solution. The mixture is stirred for a number of hours to ensure complete polymerization. Once this is done, the polypyrrole that is formed is collected and washed with de-ionized water. Then, it is sonicated twice for about 5 min, filtered using Whatman filter paper No. 1, and left to dry. This final stage results in the production of the desired polypyrrole product.

Ionomeric Membrane Preparation

The *SPVA/GO/ZnO-Nps* membrane substance was poured into a petri dish and covered with Whatman filter paper No. 1 before being placed in a thermostatically controlled oven at 60 °C for slow solvent evaporation. Once completely dried, the membrane substance was gently removed from the petri dish using forceps. It was heated at 100 °C for one hr in a

thermostatic oven to crosslink the material. After cooling to room temperature, it was discovered that the resulting ionomeric membrane was mechanically stable and ideal for actuation investigations. After that, the *SPVA/GO/ZnO-Nps* membrane was dipped in a beaker having pyrrole solution, and gently $FeCl_3$ solution was passed drop by drop within 30 min. The ratio of pyrrole and $FeCl_3$ solutions was 1:1. This caused the $FeCl_3$ to oxidize the pyrrole and create polypyrrole, resulting in a greenish–black solution. The *in-situ* polymerized membrane is processed for 5 h at an ambient temperature range of around 26 °C. The membrane is rinsed with demineralized water after 24 h and allowed to dry at the same temperature, i.e. 26 °C. Finally, for analytical purposes, the (*SPVA/GO/ZnO-Nps/PPy*) nano-composite ionic actuator is kept in distilled water at room temperature (Table 1).

Characterization of (*SPVA/GO/ZnO-Nps/PPy*) Ionomeric Membrane

Employing techniques comparable to those previously described [57], the water absorption, water loss, proton conductivity, and ion exchange capacitie of the (*SPVA/GO/ZnO-Nps/PPy*) ionomeric membrane were examined. FTIR and XRD techniques were used to analyse the (*SPVA/GO/ZnO-Nps/PPy*) nano-composite membrane's structural properties. The surface and cross-sectional morphologies of the IPMC membrane were examined using SEM. Under a sinusoidal voltage of 4 V, the maximum tip displacement and actuation force measurements of the IPMC membrane were obtained through controlled NI-PXI system, providing electro-mechanical characterizations of the investigated membrane.

Table 1 (*SPVA/GO/ZnO Nps/PPy*) polymer nano-composite membrane-based actuator: material preparation profile and ion exchange capability

S.No.	Parameters	Inputs
1	Polyvinyl alcohol	4 gm
2	4-Sulfophthalic acid	4 ml
3	Graphene oxide suspension	2 ml
4	ZnO network (nanoZO) suspension	2 ml
5	Pyrrole solution	50 ml
6	Ferric chloride ($FeCl_3$) solution	50 ml
7	Final appearance	Dark greenish–black membrane
8	Water absorption capacity	80.45%
9	Water loss	37.8%
10	Ion-exchange capacity (IEC)	1.79 meq g^{-1}
11	Proton conductivity	1.69×10^{-3} Scm^{-1}

Absorption Capacity of Water

The (*SPVA/GO/ZnO-Nps/PPy*) ionomeric membrane's capacity to absorb water was tested at ambient temperature over an array of time intervals viz. 0.5, 1, 1.5, 2, 4, 6, 8 and 24 h. To achieve this, the membranes were submerged in de-mineralized water at two distinct temperatures, namely 26 ± 3 °C as well as at 45 °C, for a duration of 24 h to facilitate water absorption. The pre-weighed dried membrane was immersed in distilled water for the aforementioned amounts of time to accomplish this. The membrane was then taken out of the water, rapidly blotted with Whatman filter paper, and weighed once more. By dividing the difference in weight between the wet and dry membranes by the dry membrane's weight, the water absorption capacity was determined using the formula shown below [57] and also in Fig. 1:

$$W = \frac{(W_{wet} - W_{dry})}{W_{dry}} \times 100 \tag{2}$$

W_{dry} is the weight of the dry membrane, while W_{wet} is the weight of the membrane after it has absorbed water.

Water Loss

The ionomeric membrane, (*SPVA/GO/ZnO-Nps/PPy*), with the highest water-absorption was weighed and exposed to an electric potential of 3–6 V for 2 to 16 min. The weight of the membrane after each time interval was recorded. The

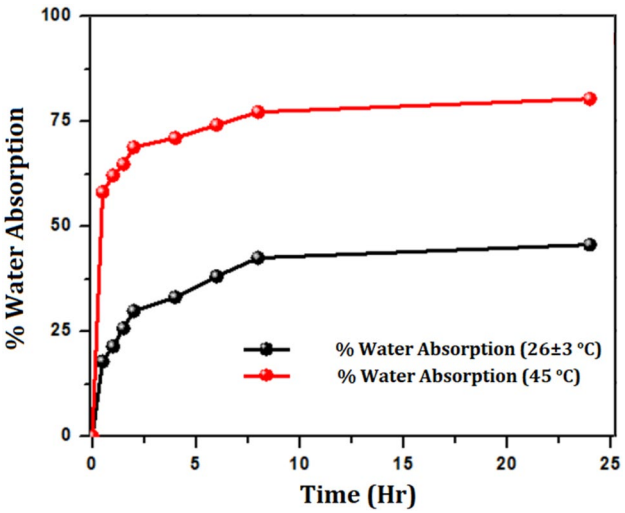

Fig. 1 Water absorption of the (*SPVA/GO/ZnO Nps/PPy*) polymer nano-composite membrane at ambient temperature of 26 ± 3 °C and at dry temperature of 45 °C

reduction in water content due to the electric potential was determined using the below formula [33] and also in Fig. 2:

$$Water\ loss\% = \frac{W_1 - W_2}{W_1} \times 100 \quad (3)$$

where W_1 and W_2 represent the wet membrane weight and the membrane weight after the water loss following the application of a voltage, respectively.

Water Loss Coupled with Voltage

The ionomeric membrane, (*SPVA/GO/ZnO-Nps/PPy*), with the highest water absorption was exposed to a voltage of 3–6 V using the potentiostat/galvanostat's linear sweep voltammetry method. The resulting voltage as well as current data were recorded.

Evaluating the Membrane's Capacity for Proton Conductivity

The impedance analyzer connected to potentiostat/galvanostat was used to determine the proton conductivity of the ionomeric membrane, (*SPVA/GO/ZnO-Nps/PPy*), with the highest water absorption and had dimensions of 1 cm width and 3 cm length. The procedure was described in previous studies. The proton conductivity (σ) was calculated using the following formula [57] (4) as:

$$\sigma = \frac{L}{R \times A} \quad (4)$$

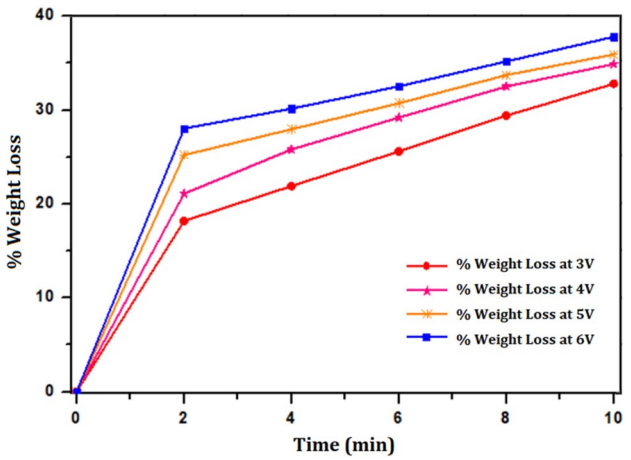

Fig. 2 Water loss of the (*SPVA/GO/ZnO Nps/PPy*) polymer nanocomposite membrane at 3–6 V DC

where σ is the proton conductivity in S cm^{-1}; L is the membrane thickness in cm; A is the area of cross-section of polymer membrane, and R is resistance.

Performance of the Ionomeric (*SPVA/GO/ZnO-Nps/PPy*) for Bending Actuation

The ionomeric membrane with the highest water absorption was exposed to voltage in the 0–6 V range, and the membrane's bending efficiency was evaluated.

Ion-exchange Capacity (IEC) of Ionomeric Membrane

Ion-exchange capacity (IEC) of the (*SPVA/GO/ZnO-Nps/PPy*) ionomeric material was measured using the classical titration method. Firstly, the ionomeric material was immersed in 1M HNO_3 for 24 h to convert it into H^+ form. It was then neutralized with distilled water and dried at 45 °C. The dried material was cut into small pieces and packed into a glass column. The ionomeric material was then converted into Na^+ form by passing 1M $NaNO_3$ through the column at a slow flow rate of 0.5 ml per min. The dissociated H^+ ions were titrated with 0.1M NaOH solution using phenolphthalein as an indicator. The IEC value of the ionomeric material in meq g^{-1} dry material was calculated using the provided formula [57] (5) as:

$$Ion-exchange\ capacity = \frac{Volume\ of\ \mathrm{NaOH}\ consumed \times Molarity\ of\ \mathrm{NaOH}}{Weight\ of\ the\ dry\ membrane} \quad (5)$$

Electro-Mechanical Analysis

In order to determine the electro-mechanical properties of the (*SPVA/GO/ZnO-Nps/PPy*) polymer nano-composite soft actuator, a test setup was established, and the basic layout for the actuation and control of the fabricated actuator is shown in Fig. 3. An experimental setup was established to determine the electro-mechanical properties of the polymer nano-composite soft actuator of (*SPVA/GO/ZnO-Nps/PPy*), and Fig. 3 shows the basic design for the actuator's actuation and regulation.

The polymeric membrane actuator, which measured roughly 30 mm by 10 mm by 0.2 mm, was fastened in a holder that was positioned in cantilever mode. A digital power supply and digital card were used to supply voltage to the actuator, and a command control operation was used to send an electrical pulse. The voltage was regulated using simple digital-to-analog card software, and the input command was sent by delivering voltage up to 6 V DC. After applying the potential, the membrane tip's

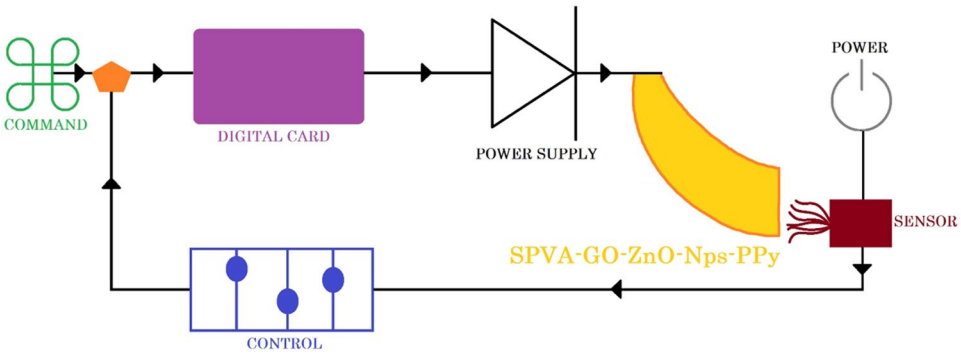

Fig. 3 Basic *GO/SPVA-nanoZO-PPy* polymer nano-composite soft actuator: control and actuation layout

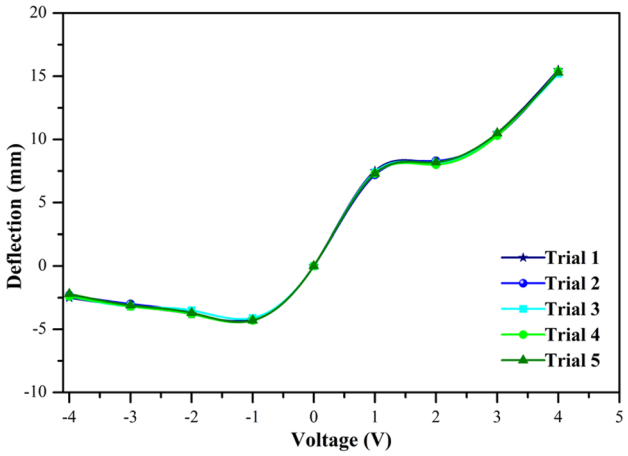

Fig. 4 (*SPVA/GO/ZnO Nps/PPy*) polymer nano-composite soft actuator stepwise exhibition of bi-directional deflection behaviour

displacement was measured using a laser-based displacement sensor, which gave feedback as the (*SPVA/GO/ZnO-Nps/PPy*) polymer nano-composite soft actuator was being operated. Figure 4 shows the bending reactions following the application of various voltages.

Table 2 presents the actuator's tip displacement data, and Fig. 5 plots its bi-directional deflection behaviour. The deflection behaviour exhibited hysteresis to some extent. The actuator's tip deflection increased as the voltage was raised, resulting in deflection faults (hysteresis), which were corrected by varying the voltage during the actuation process. The (*SPVA/GO/ZnO-Nps/PPy*) non-uniform behaviour brought on by hysteresis led the deflection under positive voltage to be somewhat larger than the equal negative voltage. By implementing control systems, this was reduced. In order to create a stable deflection, the voltage cycle was repeated ten times. Grid dimensions on the X-axis were 1 V DC and 5 mm deflection on the positive and negative sides, respectively.

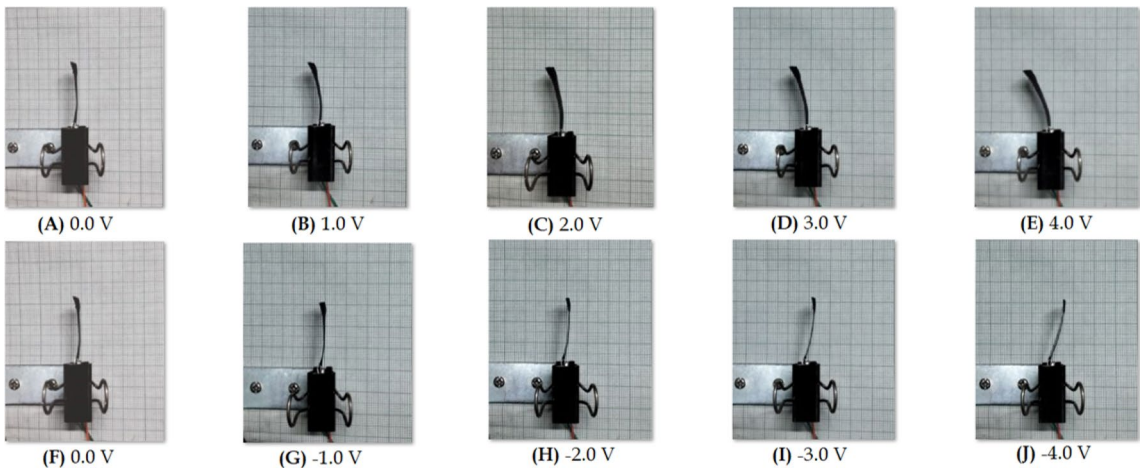

Fig. 5 Experimentally determined (*SPVA/GO/ZnO Nps/PPy*) polymer nano-composite soft actuator deflection behaviour

Table 2 Experimental deflection data of (*SPVA/GO/ZnO Nps/PPy*) polymer nano-composite soft actuator

Experimental deflection of (*SPVA/GO/ZnO Nps/PPy*) (in mm)					
Voltage (V)	0.0 V	1.0 V	2.0 V	3.0 V	4.0 V
Trial 1	0	7.5	8.2	10.5	15.5
Trial 2	0	7.2	8.3	10.3	15.4
Trial 3	0	7.4	8.1	10.4	15.2
Trial 4	0	7.3	8.0	10.3	15.4
Trial 5	0	7.3	8.2	10.5	15.3

Result and Discussion

This section discusses the findings related to the water absorption, water loss, proton conductivity, and ion exchange capacities of the (*SPVA/GO/ZnO-Nps/PPy*) polymer nano-composite soft actuator. The results of these tests are presented and analyzed. Additionally, the electro-mechanical properties of the actuators are described in detail. The section also presents the results of FTIR, XRD, and SEM analyses conducted to assess the surface and cross-sectional morphologies of the IPMNC. The findings from these tests are discussed, highlighting any noteworthy observations and insights gained from the analyses. Overall, this section aims to provide a comprehensive understanding of the various properties and characteristics of the (*SPVA/GO/ZnO-Nps/PPy*) polymer nano-composite soft actuator.

Water Absorption, Water Loss, Proton Conductivity, and Ion Exchange Capacities of the (*SPVA/GO/ZnO-Nps/PPy*)

The Ion-exchange capacity (IEC) of the (*SPVA/GO/ZnO-Nps/PPy*) polymer nano-composite ionomeric membrane is a crucial factor in determining how efficiently protons can transfer through the ionic channels/sites in the IPMC membrane, which ultimately impacts the actuator's performance. The IEC of the membrane was evaluated and found to be approximately 1.79 meq g^{-1}. The adequate IEC value of the IPMC membrane allows for increased water absorption capacity and more PPy fixation on both sides of the surfaces of the membrane. This uniform loading of PPy on the membrane's surface reduces its resistance and, therefore, can lead to better bending performance. The water loss and water absorption capacities of the (*SPVA/GO/ZnO-Nps/PPy*) polymer nano-composite ionomeric membrane were also evaluated, and the results indicate that the membrane can retain approximately 37.8% of water at 6 V for 10 min and absorb around 80.45% of water at 45 °C for 24 h. These findings provide useful information regarding the membrane's ability to retain water and its impact on the actuator's performance.

In an ionomeric membrane, proton conductivity signifies the passage of protons (H^+ ions) within its structure. This property serves as an indicator of the membrane's proficiency in facilitating proton transfer, which, in turn, plays a pivotal role in determining the membrane's actuation capacity. For the polymer nano-composite ionomeric membrane *(SPVA/GO/ZnO-Nps/PPy)*, the measured proton conductivity was determined to be 1.6 mS cm^{-1}, which demonstrates a notably elevated value in comparison to the data presented in Table 4 from prior studies [40, 57].

A high value of proton conductivity means that the excess H^+ ions in their hydrated form can easily migrate through the membrane, resulting in a good actuation capacity. This property is crucial for the membrane's ability to respond to electrical stimuli and bend in a controlled manner.

FTIR Analysis

Figure 6a, b show the Fourier transform infrared spectroscopy (FTIR) spectra of the investigated (*SPVA/GO/ZnO-Nps/PPy*) polymer nano-composite ionomeric membrane and (*SPVA/GO/ZnO-Nps*) membrane, respectively. The FTIR spectra of the membrane in the range of 400–4000 cm^{-1} revealed the presence of functional groups such as GO, $–SO_3H$, PVA, and PPy. The characteristic peaks corresponding to the functional groups present in each component were observed. For example, the peaks located around 1050–1150 cm^{-1} and 1600–1700 cm^{-1} corresponded to the C–O–C stretching and C=O stretching vibrations, respectively, of the sulphonated PVA. A peak at around 3400 cm^{-1} corresponded to the O–H stretching vibration of the PVA hydroxyl groups.

The FTIR spectrum of nanosized ZnO network (*ZnO-Nps*) showed a weak peak at around 400–600 cm^{-1} corresponding to the Zn–O bond stretching vibration. For GO, the characteristic peaks were located around 1000–1100 cm^{-1} (C–O stretching vibration), 1200–1400 cm^{-1} (C–O–C stretching vibration), and 1600–1700 cm^{-1} (C=C stretching vibration). Polypyrrole (PPy) displayed a peak at around 1550 cm^{-1} corresponding to the C=N stretching vibration of the pyrrole ring and another peak at around 1460 cm^{-1} corresponding to the C=C stretching vibration of the pyrrole ring. FTIR can provide useful information about the functional groups present in each component and the interactions between the components. There may be additional peaks or shifts in peak position due to chemical interactions between the components. Figure 6 illustrates the FTIR spectra of the (*SPVA/GO/ZnO-Nps/PPy*) membrane, revealing the functional groups that are present [58, 59].

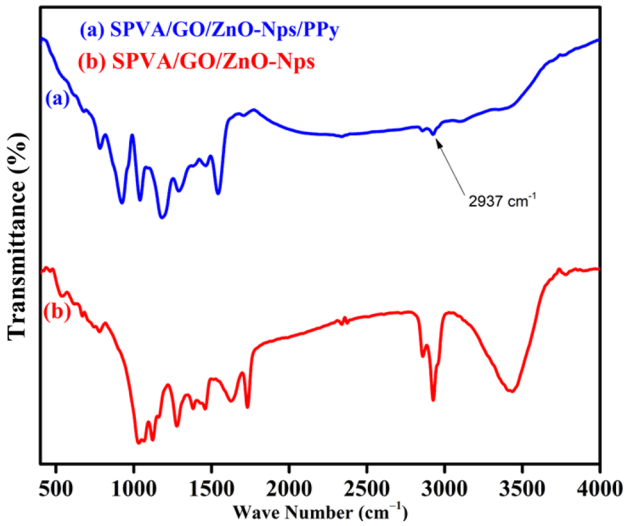

Fig. 6 FTIR spectrum of the synthesized (*SPVA/GO/ZnO Nps/PPy*) polymer nano-composite membrane

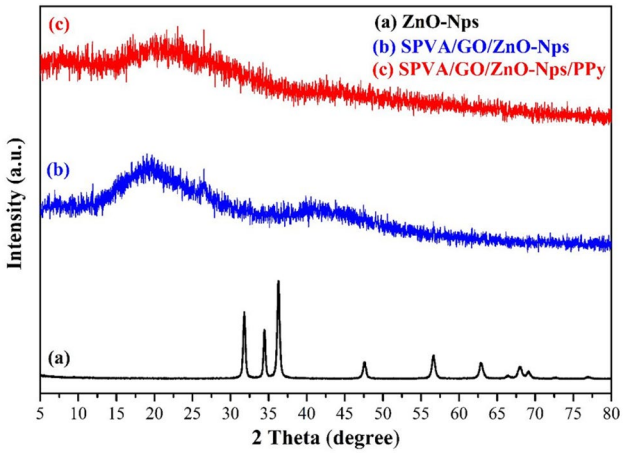

Fig. 7 XRD patterns of the synthesized (*SPVA/GO/ZnO Nps/PPy*) polymer nano-composite membrane

XRD Analysis

X-Ray diffraction analysis (XRD) is a non-invasive method that offers comprehensive insights into a material's crystalline framework, chemical formulation, and physical characteristics. Figure 7 illustrates the X-ray diffraction (XRD) spectra of three distinct materials: ZnO network (ZnO-Nps) in Fig. 7a. Subsequently, the XRD spectra of the ionomeric membrane are then shown in Fig. 7b, c, in the absence and presence of polypyrrole (PPy), respectively. The spectrum of ZnO-Nps shown in Fig. 7a exhibits diffraction peaks that closely mimic the distinctive pattern of normal hexagonal wurtzite ZnO [55, 57]. Strong and distinct peaks in the spectrum suggest that the generated nanoflower sample has a highly crystalline shape. The obtained spectrum of ZnO-Nps displayed no evident additional peaks attributed to impurities.

Furthermore, as in Fig. 7b, the XRD pattern of SPVA/GO/ZnO Nps showed a broad peak of GO observed around $2\theta = 10° - 25°$, corresponding to the (002) plane of the graphene oxide. In addition, sulphonated PVA peaks can be observed at around $2\theta = 10° - 20°$, corresponding to the (110) and (200) planes of PVA, respectively. X-ray diffraction (XRD) investigation of the (*SPVA/GO/ZnO Nps/PPy*) polymer nano-composite ionomeric membrane revealed the existence of numerous additional phases in addition to ZnO-Nps. A broad peak at $2\theta = 25° - 35°$ corresponds to the polypyrrole (PPy) is also seen in the spectrum. Compared to the prominent ZnO-Nps peaks, these detected peaks for the other phases showed considerably lower intensities. In the case of the (*SPVA/GO/ZnO Nps/PPy*) polymer nanocomposite ionomeric membrane, XRD analysis can provide information about the structural properties of each component in the membrane and the interactions between the components. Finally, the (*SPVA/GO/ZnO Nps/PPy*) polymer nanocomposite ionomeric membrane was shown to be amorphous in these XRD spectrum examinations [60].

SEM Analysis

Scanning electron microscopy (SEM) is a technique used to observe the surface morphology and microstructure of materials with an operating voltage of 200 kV using a JSM 6510 LV equipment made by JEOL in Japan. In the case of (*SPVA/GO/ZnO-Nps/PPy*) polymer nano-composite ionomeric membrane made of GO, Sulphonated PVA, ZnO network (*ZnO-Nps*) and Polypyrrole, the sample is first coated with a thin layer of conductive material, typically gold or carbon, to prevent charging of the surface during imaging. The coated sample is then placed in the SEM, where a focused beam of electrons is scanned over the surface. The electrons interact with the sample, producing secondary electrons, backscattered electrons, and other signals that can be detected and used to generate an image. In the case of nanocomposites, SEM can reveal the morphology of the nanoflowers, the distribution of the graphene oxide, and the overall structure of the composite as per the SEM micrograph shown in Fig. 8a; upper surface in Fig. 8b and also the cross-sectional presentation in Fig. 8c, d. The image resolution is typically on the order of nanometers, allowing for detailed examination of the composite structure.

The (*SPVA/GO/ZnO-Nps/PPy*) polymer nano-composite ionomeric membrane's surface and cross-sectional morphologies are depicted in Fig. 8a–d. At 1000× magnifications, Fig. 8a, b display the membrane's surface morphology and illustrate the flower-shaped (ZnO-Nps) dispersed in the matrix of the membrane. On the other hand, Fig. 8c, d, respectively, display the surface and cross-sectional views at 200× and 100× magnification. The flower-shaped (*ZnO-Nps*)

coating is evident on the membrane surface, while the cross-sectional images show two boundaries: the PPy membrane's outer layer and the inner membrane, which is highlighted in Fig. 8d. The Pt coating's thickness is approximately 137 µm, and the whole IPMC membrane is approximately 226 µm thick. These images demonstrate the successful coating of the (*SPVA/GO/ZnO-Nps*) membrane with *PPy*.

EDX Analysis

Figure 9 represents the elemental composition of the synthesized polymer nanocomposite membrane; it was investigated during the SEM analysis to confirm the expected elements in the membrane. The elemental mapping, as shown in Fig. 9a–f, illustrates that Nitrogen (N), Carbon (C), Oxygen (O), Sulphur (S), and Zinc (Zn) elements are present in the sample. The elemental analysis shows that the 'N' element is uniformly distributed in the sample, confirming the successful PPy coating over the membrane. Moreover, energy dispersive X-ray (EDX) reveals all the elements' peaks present in mapping, as shown in Fig. 9g. This outcome further strengthens successful synthesis of the polymer nanocomposite membrane (*SPVA/GO/ZnO-Nps/PPy*).

Electro-Mechanical Analysis

An experimental setup is established for characterizing the electro-mechanical behavior of the (*SPVA/GO/ZnO-Nps/PPy*) polymer nano-composite membrane-based actuator. The customized control system produces the 0–4 V DC which is sent to the (*SPVA/GO/ZnO-Nps/PPy*) polymer nano-composite membrane-based actuator through command control input software as depicted in Fig. 3. During supplying the voltage (0–4 V DC), the successive bending behaviour at different voltages is achieved. The deflection is noted in the interval of 1 V DC. Several trials are conducted and the data of tip deflection of the (*SPVA/GO/ZnO-Nps/PPy*) polymer nano-composite membrane-based actuator are given in Table 2.

Finding the force behaviour of the (*SPVA/GO/ZnO-Nps/PPy*) polymer nano-composite membrane-based actuator, a mini/digital load weighing scale is utilized to measure the force data of the (*SPVA/GO/ZnO-Nps/PPy*) polymer nano-composite membrane-based actuator (Make: Citizen, model: CX220, Make: India). The voltage range (0–4 V DC) is applied to the actuator. During experimentation, the (*SPVA/GO/ZnO-Nps/PPy*) polymer nano-composite membrane-based actuator is put in a horizontal cantilever mode so that the tip of the polymer actuator will touch the pan surface of the load cell by applying controlled voltage. Several trials (5 Nos) are conducted and the experimental data are given in Table 3; Fig. 10. Through experimentation, it is envisaged that the maximum load by this actuator can attain up to 0.2420 mN as shown in Fig. 10. During experimentation, the error of the (*SPVA/GO/ZnO-Nps/PPy*) polymer nano-composite membrane-based actuator has also been diminished and it also reveals the excellent repeatability of the force behaviour. The repeatability of this actuator is achieved up to 81.06%. In Fig. 11, the normal distribution for the (*SPVA/GO/ZnO-Nps/PPy*) polymer nano-composite membrane-based actuator is displayed, where the standard deviation of the average force (F) and the mean values are used to generate the distribution. This distribution indicates the behaviour of the force characteristics of the actuator, specifically its repeatability and sharpness. The sharp shape of the distribution indicates that the force characteristics of the actuator are consistent and have a small degree of variability. Additionally, the good repeatability behaviour of the force characteristics suggests that the actuator can consistently produce the same level of force across multiple trials, indicating its reliability. The comparison of different properties with different kind of IPMCs

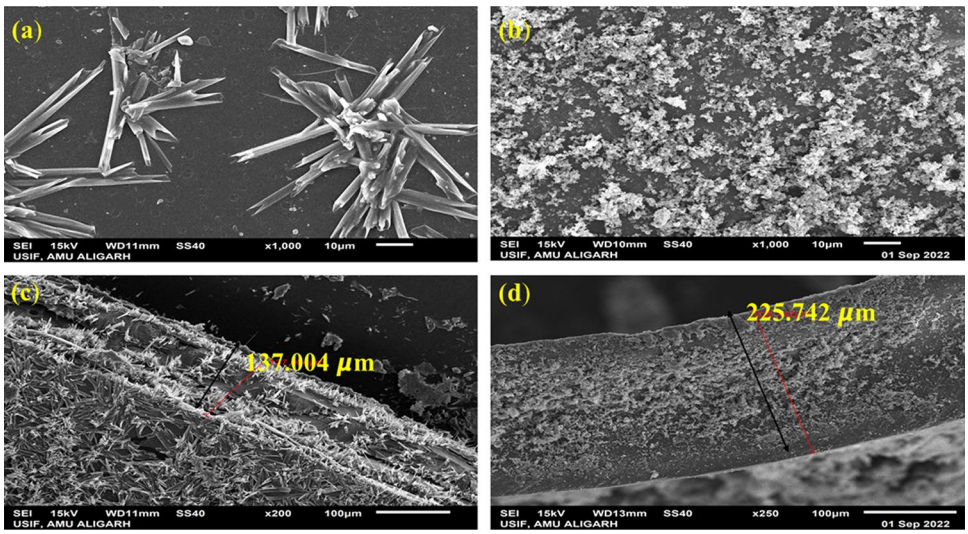

Fig. 8 SEM images of the synthesized (*SPVA/GO/ZnO Nps/PPy*) polymer nano-composite membrane

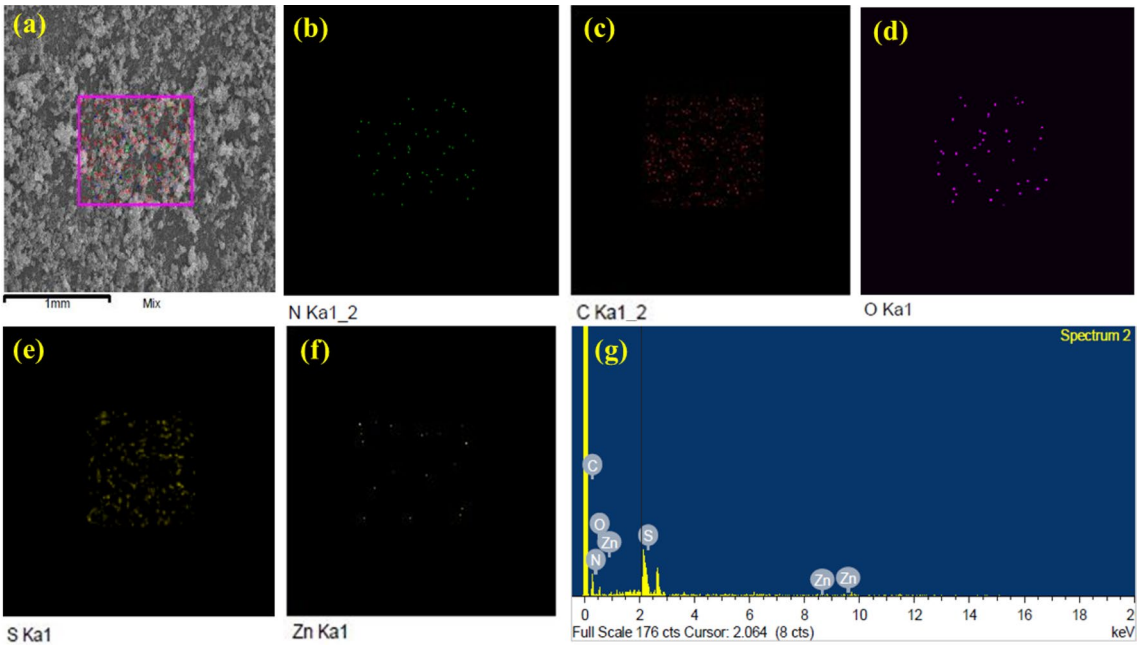

Fig. 9 Represent the images of **a** mapping of the synthesized (*SPVA/GO/ZnO Nps/PPy*) polymer nano-composite membrane **b** element Nitrogen (N); **c** element Carbon (C); **d** element Oxygen (O); **e** element Sulfur (S); **f** element Zinc (Zn) and **g** EDX spectrum shows characteristic peaks of all the expected elements present in (*SPVA/GO/ZnO Nps/PPy*) polymer nano-composite membrane

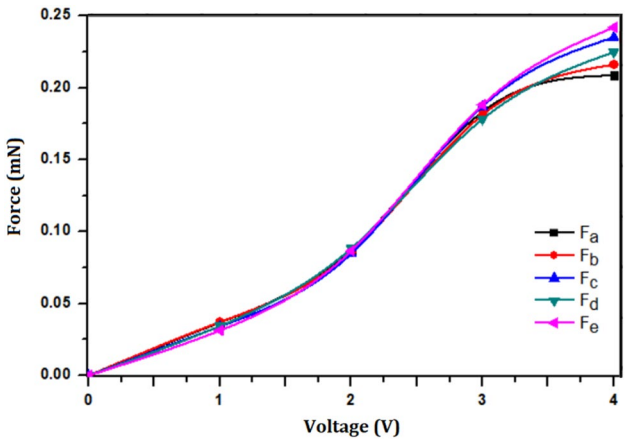

Fig. 10 Experimental force behaviour of (*SPVA/GO/ZnO Nps/PPy*) polymer nano-composite membrane actuator

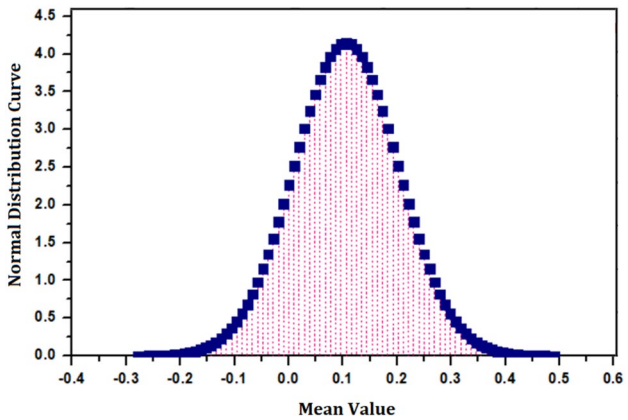

Fig. 11 Normal distribution curve of (*SPVA/GO/ZnO Nps/PPy*) polymer nano-composite membrane actuator

is summarized in Table 4. It shows that the properties of the (*SPVA/GO/ZnO-Nps/PPy*) polymer nano-composite membrane actuator is almost better than other types of IPMC based on different components of the membrane materials. Table 4 provides a comparison of various properties among different types of IPMCs. The results indicate that the *(SPVA/GO/ZnO-Nps/PPy)* polymer nano-composite membrane based-actuator exhibits competent properties compared to other IPMCs that employ different membrane materials.

Conclusions

The main objective of this article is to present a new type of actuator i.e. (*SPVA/GO/ZnO-Nps/PPy*) polymer nano-composite membrane-based actuator, and elaborate on its development and distinctive properties. To investigate the actuator's structural, morphological, and electro-mechanical features, various techniques were employed. The results indicate that the actuator has good actuation performance, including force and tip deflection/displacement, as well

Table 3 Force data of (*SPVA/GO/ZnO Nps/PPy*) polymer nano-composite membrane actuator

Force data of (*SPVA/GO/ZnO Nps/PPy*) (in mN)						
Voltage	F_a	F_b	F_c	F_d	F_e	Average force (F)
0.0 V	0	0	0	0	0	0
1.0 V	0.0369	0.0372	0.0341	0.0344	0.0313	0.0348
2.0 V	0.0875	0.0858	0.0847	0.0884	0.0867	0.0866
3.0 V	0.1833	0.1812	0.1870	0.1782	0.1882	0.1836
4.0 V	0.2087	0.2162	0.2351	0.2249	0.2420	0.2254
Mean						0.106
Standard deviation						0.086
Repeatability						81.06%

Table 4 Comparison of (*SPVA/GO/ZnO Nps/PPy*) polymer nano-composite membrane-based actuator with other IPMC actuators

Properties	(*SPVA/GO/ZnO Nps/PPy*)	SPEES/PVDF/ SGO/Pt [40]	Sulfonated polyvinyl alcohol/Py [57]	Kraton/GO/ Ag/Pani [58]	Nafion based IPMC [61]
Water absorption (%)	80.45	78	82.3	314	16.70
Tip displacement (mm)	15.5	15.2	18.5	17.5	12
Ion-exchange capacity (meq g^{-1})	1.79	1.95	1.2	1.88	0.98
Proton conductivity (Scm $^{-1}$)	1.69×10^{-3}	1.62×10^{-2}	1.6×10^{-3}	1.302×10^{-3}	9.0×10^{-3}

as repeatability with the (*SPVA/GO/ZnO-Nps/PPy*) polymer nano-composite membrane. Furthermore, the actuator exhibits a high capacity for proton conductivity and water absorption, a low water loss rate, and a high ion-exchange capacity under applied electric potential. The electromechanical analysis reveals that the newly developed nanocomposite membranes can be used to handle soft objects. Consequently, this discovery has the potential to pave the way for the creation of a micro-gripping system for soft robotic applications using the identified membrane.

Acknowledgements The Department of Chemistry, Faculty of Science, University of Tabuk, Saudi Arabia, provided the authors with enthusiastic support for their present study, which they would like to acknowledge.

Author Contributions Conceptualization, SKM, MMHAJ.; methodology, SKM, MMHAJ, AHA, and HAAA; software, SKM, MMHAJ, AHA, MAA, NO and AOA; validation, SKM, MMHAJ, AHA., and HAAA; data analysis; SKM, MMHAJ, AHA, MAA, NO and AOA; writing—original draft preparation, SKM, MMHAJ, AHA., and HAAA; writing—review and editing, SKM, MMHAJ, AHA, HAAA, FA; visualization, SKM, MMHAJ, AHA, and HAAA; supervision, SKM, MMHAJ, AHA, HAAA and FA; project administration, SKM, MMHAJ, AHA, and HAAA. All authors have read and agreed to the published version of the manuscript.

Funding Not applicable.

Data Availability Not applicable.

Declarations

Conflict of interest The authors declare that the research was conducted in the absence of any commercial or financial relationships that could be construed as a potential conflict of interest.

References

1. Kim HM, Vinh ND (2019) Study on Time-Dependent bending response of IPMC Actuator. Ionic polymer metal composites for sensors and actuators. Springer, Cham, pp 75–138
2. Qaviandam Z, Naghavi N, Safaie J (2020) A new approach to improve IPMC performance for sensing dynamic deflection: sensor biasing. IEEE Sens J 20(15):8614–8622
3. Annabestani M, Naghavi N, Maymandi-Nejad M (2021) A 3D analytical ion transport model for ionic polymer metal composite actuators in large bending deformations. Sci Rep 11(1):1–15
4. He Q, Liu Z, Yin G, Yue Y, Yu M, Li H, Ji K, Xu X, Dai Z, Chen M (2020) The highly stable air-operating ionic polymer metal composite actuator with consecutive channels and its potential application in soft gripper. Smart Mater Struct 29(4):045013
5. He Z, Jiao S, Wang Z, Wang Y, Yang M, Zhang Y, Liu Y, Wu Y, Shang J, Chen Q, Li RW (2022) An antifatigue liquid metal composite electrode ionic polymer-metal composite artificial muscle with excellent electromechanical properties. ACS Appl Mater Interfaces 14(12):14630–14639
6. Hao M, Wang Y, Zhu Z, He Q, Zhu D, Luo M (2019) A compact review of IPMC as soft actuator and sensor: current trends, challenges, and potential solutions from our recent work. Front Rob AI 6:129
7. Chen Z (2017) A review on robotic fish enabled by ionic polymer–metal composite artificial muscles. Rob Biomimetics 4(1):1–13

8. Weder C (2021) ACS macro letters–your go-to journal for research on stimuli-responsive polymers. ACS Macro Lett 10(11):1450–1453
9. MohdIsa W, Hunt A, HosseinNia SH (2019) Sensing and self-sensing actuation methods for ionic polymer–metal composite (ipmc): a review. Sensors 19(18):3967
10. Sideris EA, de Lange HC, Hunt A (2020) An ionic polymer metal composite (ipmc)-driven linear peristaltic microfluidic pump. IEEE Rob Autom Lett 5(4):6788–6795
11. Graziani S (2015) Ionic polymer metal composites as post-silicon transducers for the realisation of smart systems. In: Ionic polymer metal composites (IMPCs): smart multi-functional materials and artificial muscles, vol 2. p 158
12. Shahinpoor M (2009) Implantable heart-assist and compression devices employing an active network of electrically-controllable ionic polymer-metal nanocomposites. Biomedical applications of electroactive polymer actuators. Wiley, Chichester, pp 137–160
13. Yue C, Guo S, Li Y, Li M (2014) Bio-inspired robot launching system for a mother-son underwater manipulation task. In 2014 IEEE International Conference on Mechatronics and Automation. IEEE, pp. 174–179
14. Ruth D (2019) Robotic assemblies based on IPMC actuator. Ionic Polym Metal Compos Sens Actuators. Springer, Cham, pp 183–194
15. Jain RK, Hussain S, Naushad M (2015) Poly (3, 4-ethylenedioxythiophene): polystyrene sulfonate zirconium (iv) phosphate (PEDOT: PSS–ZrP) composite ionomeric membrane for artificial muscle applications. RSC Adv 5(103):84526–84534
16. Nguyen VK, Yoo Y (2007) A novel design and fabrication of multilayered ionic polymer-metal composite actuators based on Nafion/layered silicate and Nafion/silica nanocomposites. Sens Actuators B 123(1):183–190
17. Wang J, McDaid A, Sharma R, Aw KC (2015) A compact ionic polymer metal composite (IPMC) system with inductive sensor for closed loop feedback. Actuators 4(2):114–126
18. Wu D, Yang Z, Sun H (2009) Vibration control efficiency of piezoelectric shunt damping system. Front Mech Eng China 4(4):441–446
19. Tsai TH, Ertem SP, Maes AM, Seifert S, Herring AM, Coughlin EB (2015) Thermally cross-linked anion exchange membranes from solvent processable isoprene containing ionomers. Macromolecules 48(3):655–662
20. Kusoglu A, Weber AZ (2017) New insights into perfluorinated sulfonic-acid ionomers. Chem Rev 117(3):987–1104
21. Feng T, Lin B, Zhang S, Yuan N, Chu F, Hickner MA, Wang C, Zhu L, Ding J (2016) Imidazolium-based organic–inorganic hybrid anion exchange membranes for fuel cell applications. J Membr Sci 508:7–14
22. Panwar V, Cha K, Park JO, Park S (2012) High actuation response of PVDF/PVP/PSSA based ionic polymer metal composites actuator. Sens Actuators B 161(1):460–470
23. Oh C, Kim S, Kim H, Park G, Kim J, Ryu J, Li P, Lee S, No K, Hong S (2019) Effects of membrane thickness on the performance of ionic polymer–metal composite actuators. RSC Adv 9(26):14621–14626
24. Ru J, Zhu Z, Wang Y, Chen H, Li D (2018) Tunable actuation behavior of ionic polymer metal composite utilizing carboxylated carbon nanotube-doped Nafion matrix. RSC Adv 8(6):3090–3094
25. He Q, Yu M, Li Y, Ding Y, Guo D, Dai Z (2012) Investigation of ionic polymer metal composite actuators loaded with various tetraethyl orthosilicate contents. J Bionic Eng 9(1):75–83
26. Wang J, Xu C, Taya M, Kuga Y (2008) April. Bio-inspired tactile sensor with arrayed structures based on electroactive polymers. Electroactive Polymer Actuators and Devices (EAPAD) 2008 6927:402–409
27. Tabatabaie SE (2019) Novel configurations of ionic polymer-metal composites (IPMCs) as sensors, actuators, and Energy Harvesters. The University of Maine
28. Stalbaum T, Trabia S, Hwang T, Olsen Z, Nelson S, Shen Q, Lee DC, Kim KJ, Carrico J, Leang KK, Palmre V (2018) Guidelines for making ionic polymer–metal composite (IPMC) materials as artificial muscles by advanced manufacturing methods: state of the art. In: Advances in manufacturing and processing of materials and structures. pp 377–394
29. Liu Q, Li Z, Wang D, Li Z, Peng X, Liu C, Zheng P (2020) Metal organic frameworks modified proton exchange membranes for fuel cells. Front Chem 8:694
30. Anahidzade N, Abdolmaleki A, Dinari M, Tadavani KF, Zhiani M (2018) Metal-organic framework anchored sulfonated poly (ether sulfone) as a high temperature proton exchange membrane for fuel cells. J Membr Sci 565:281–292
31. ul Haq M, Gang Z (2016) Ionic polymer–metal composite applications. Emerg Mater Res 5(1):153–164
32. Luqman M, Shaikh H, Anis A, Al-Zahrani SM, Hamidi A (2022) Platinum-coated silicotungstic acid-sulfonated polyvinyl alcohol-polyaniline based hybrid ionic polymer metal composite membrane for bending actuation applications. Sci Rep 12(1):1–9
33. Khan A, Luqman M, Dutta A (2014) Kraton based ionic polymer metal composite (IPMC) actuator. Sens Actuators A: Phys 216:295–300
34. Luqman M, Shaikh HM, Anis A, Al-Zahrani SM, Alam MA (2022) A convenient and simple ionic polymer-metal composite (IPMC) actuator based on a platinum-coated sulfonated poly (ether ether ketone)–polyaniline composite membrane. Polymers 14(4):668
35. Jain RK, Khan A, Asiri AM (2019) Design and development of non-perfluorinated ionic polymer metal composite-based flexible link manipulator for robotics assembly. Polym Compos 40(7):2582–2593
36. Luqman M, Lee JW, Moon KK, Yoo YT (2011) Sulfonated polystyrene-based ionic polymer–metal composite (IPMC) actuator. J Ind Eng Chem 17(1):49–55
37. Wang J, Wang Y, Zhu Z, Wang J, He Q, Luo M (2019) The effects of dimensions on the deformation sensing performance of ionic polymer-metal composites. Sensors 19(9):2104
38. Inamuddin E, Mohammad A, Asiri AM (2016) New polymeric composite materials. Materials Research Forum LLC, Millersville
39. Mehraeen S, Sadeghi S, Cebeci F, Papila M, Gürsel SA (2018) Polyvinylidene fluoride grafted poly (styrene sulfonic acid) as ionic polymer-metal composite actuator. Sens Actuators A: Phys 279:157–167
40. Khan A, Jain RK, Ghosh B, Asiri AM (2018) Novel ionic polymer–metal composite actuator based on sulfonated poly (1,4-phenylene ether-ether-sulfone) and polyvinylidene fluoride/sulfonated graphene oxide. RSC Adv 8(45):25423–25435
41. Hwang T, Palmre V, Nam J, Lee DC, Kim KJ (2015) A new ionic polymer–metal composite based on Nafion/poly (vinyl alcohol-co-ethylene) blends. Smart Mater Struct 24(10)
42. Khan A, Jain RK (2016) Easy, operable ionic polymer metal composite actuator based on a platinum-coated sulfonated poly (vinyl alcohol)–polyaniline composite membrane. J Appl Polym Sci. https://doi.org/10.1002/app.43787
43. Motealleh B, Huang F, Largier TD, Khan W, Cornelius CJ (2019) Solution-blended sulfonated polyphenylene and branched poly (arylene ether sulfone): synthesis, state of water, surface energy, proton transport, and fuel cell performance. Polymer 160:148–161
44. Wang D, Cornelius CJ (2017) Modeling ionomer swelling dynamics of a sulfonated polyphenylene, pentablock copolymers, and nafion. J Polym Sci Part B: Polym Phys 55(5):435–443
45. Zhao Y, Xu D, Sheng J, Meng Q, Wu D, Wang L, Xiao J, Lv W, Chen Q, Sun D (2018) Biomimetic beetle-inspired flapping air

vehicle actuated by ionic polymer-metal composite actuator. Appl Bionics Biomech. https://doi.org/10.1155/2018/3091579
46. Jain RK (2021) Development of different types of ionic polymer metal composite-based soft actuators for robotics and biomimetic applications. Soft Robotics in Rehabilitation. Academic Press, Cambridge, pp 39–87
47. Stoimenov BL, Rossiter JM, Mukai T (2007) Manufacturing of ionic polymer-metal composites (IPMCs) that can actuate into complex curves. Electroact Polym Actuators Devices (EAPAD) 2007 6524:234–244
48. Tepermeister M, Bosnjak N, Dai J, Zhang X, Kielar SM, Wang Z, Tian Z, Suntivich J, Silberstein MN (2022) Soft ionics: governing physics and state of technologies. Front Phys. https://doi.org/10.3389/fphy.2022.890845
49. Khan A, Jain RK, Naushad M (2015) Fabrication of a silver nano powder embedded kraton polymer actuator and its characterization. RSC Adv 5(111):91564–91573
50. Masoomi MY, Morsali A (2012) Applications of metal–organic coordination polymers as precursors for preparation of nanomaterials. Coord Chem Rev 256(23–24):2921–2943
51. Jung Y, Kim SJ, Kim KJ, Lee DY (2011) Characteristics of ionic polymer–metal composite with chemically doped TiO_2 particles. Smart Mater Struct 20:124004
52. Oh IK, Jung JY (2008) Biomimetic nano-composite actuators based on carbon nanotubes and ionic polymers. J Intell Mater Syst Struct 19(3):305–311
53. Fang BK, Ju MS, Lin CCK (2007) A new approach to develop ionic polymer–metal composites (IPMC) actuator: fabrication and control for active catheter systems. Sens Actuators A: Phys 137(2):321–329
54. Chung CK, Fung PK, Hong YZ, Ju MS, Lin CCK, Wu TC (2006) A novel fabrication of ionic polymer-metal composites (IPMC) actuator with silver nano-powders. Sens Actuators B 117(2):367–375
55. Khan MF, Hameedullah M, Ansari AH, Ahmad E, Lohani MB, Khan RH, Alam MM, Khan W, Husain FM, Ahmad I (2014) Flower-shaped ZnO nanoparticles synthesized by a novel approach at near-room temperatures with antibacterial and antifungal properties. Int J Nanomed 9:853
56. Cullity BD (1956) Elements of X ray diffraction. Addison-Wesley Publishing Company, Reading
57. Khan A, Jain RK, Naushad M (2015) Development of sulfonated poly (vinyl alcohol)/polpyrrole based ionic polymer metal composite (IPMC) actuator and its characterization. Smart Mater Struct 24(9):095003
58. Khan A, Jain RK, Banerjee P, Asiri AM (2017) Soft actuator based on Kraton with GO/Ag/Pani composite electrodes for robotic applications. Mater Res Express 4(11):115701
59. Ahamed MI, Inamuddin Asiri AM, Luqman M, Lutfullah, (2019) Preparation, physicochemical characterization, and microrobotics applications of polyvinyl chloride- (PVC-) based PANI/PEDOT: PSS/ZrP composite cation-exchange membrane. Adv Mater Sci Eng 2019:1–11
60. Luqman M, Anis A, Shaikh HM, Al-Zahrani SM, Alam MA (2022) Development of a soft robotic bending actuator based on a novel sulfonated polyvinyl chloride-phosphotungstic acid ionic polymer-metal composite (IPMC) membrane. Membranes 12(7):651
61. Zawodzinski TA, Derouin C, Radzinski S, Sherman RJ, Smith VT, Springer TE, Gottesfeld S (1993) Water uptake by and transport through Nafion® 117 membranes. J Electrochem Soc 140(4):1041